J. Fluid Mech. (1979), *vol.* 95, *part* 4, *pp.* 609–633
Printed in Great Britain

Mathematical modelling of three-dimensional heated surface jets

By J. J. McGUIRK† AND W. RODI
Sonderforschungsbereich 80, University of Karlsruhe, Germany

(Received 15 December 1978)

A new economical finite-difference method is described for the calculation of three-dimensional heated surface jets discharging into stagnant water. The equations solved are for continuity, lateral and longitudinal momentum, and thermal energy. The turbulent shear stresses and heat fluxes in these equations are determined with a turbulence model involving simplified forms of the transport equations for these stresses and fluxes and the solution of differential transport equations for the turbulent kinetic energy k and the rate of its dissipation ϵ. The experimentally observed entrainment reduction due to buoyancy is reproduced by this model. The predictions are compared in detail with the recent measurements of Pande & Rajaratnam, which are judged to be superior to those of other investigators. The agreement is generally satisfactory.

1. Introduction

1.1. *Problem background*

The continuing increase in electric power generation and the accompanying increase in power plant size have intensified the problem of removal of the waste heat rejected by the generating plants. By far the cheapest way of removing waste heat is the once-through cooling method in which cooling water is first withdrawn from a natural water body and then returned to it after heating. Even though it is in certain countries only seldom adopted for new power stations owing to its ecological hazards, this method is still of great practical relevance because it is used in most existing power stations and also because other countries will continue to rely on it for economical reasons. Hence there is still a considerable interest in the performance of large heated water discharges into rivers, lakes and coastal regions, and, for design and monitoring purposes, also a great need for methods with which the impact of such discharges on the natural water body can be calculated.

The cheapest and therefore most popular way of discarding the heated water is by means of a canal or channel discharging at the water surface. The behaviour of such discharges into rivers, lakes or coastal regions is in general influenced by many complicating features like cross flow, bottom interference, or unsteadiness due to tidal or wind effects. This paper is concerned with a calculation method for the special but still relevant case of a heated surface discharge where none of these features are present, i.e. the case of a discharge into a stagnant, deep lake.

The flow situation considered is sketched in figure 1: heated water of temperature

† Present address: Department of Chemical Engineering, Imperial College, London.

0022-1120/79/4323-7640 $02.00

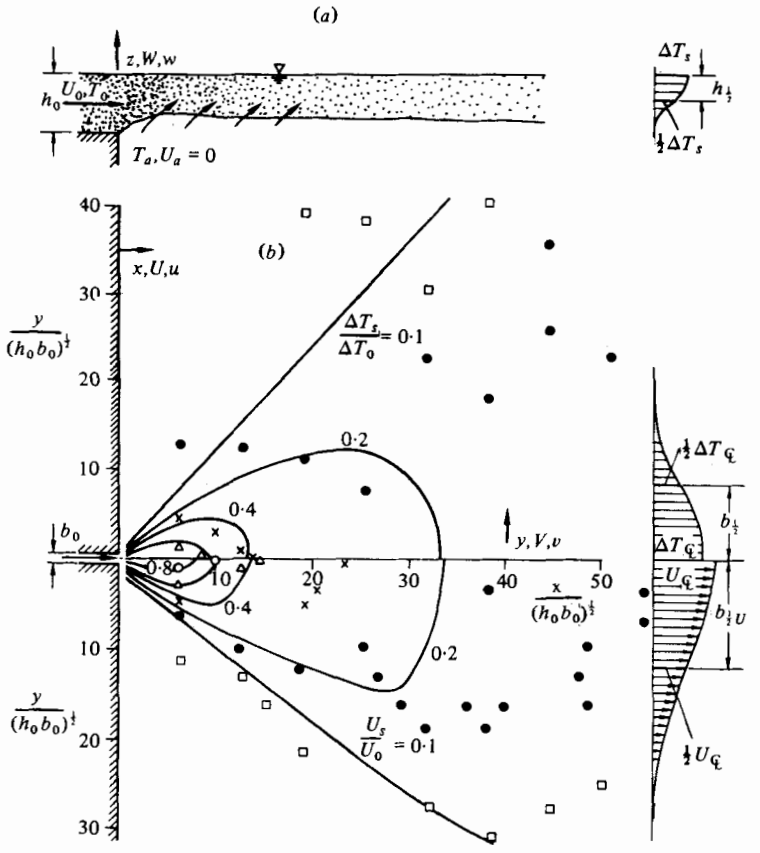

FIGURE 1. Flow configuration and surface isotherms and isotachs for run 1 ($F_0 = 2{\cdot}56$). (*a*) Sectional view; (*b*) plan view. Experimental results (Pande & Rajaratnam 1975), $\Delta T_s/\Delta T_0$, U_s/U_0: ○, 0·8; △, 0·6; ×, 0·4; ●, 0·2; □, 0·1; ——, predicted.

T_0 is discharged from a rectangular surface outlet of width b_0 and depth h_0 into an infinitely large stagnant body of water at ambient temperature T_a. A warm water jet develops whose spreading is governed by the actions of both turbulence and buoyancy. The lateral spreading is almost entirely due to buoyancy and is much larger than that of a non-buoyant jet; the vertical spreading on the other hand is much smaller for two reasons. Firstly, buoyancy induces an upward motion counteracting vertical spreading, and secondly the vertical entrainment (and thus the turbulent spreading) is reduced by buoyancy. The dilution of the heated water is almost entirely due to vertical entrainment; lateral entrainment at the sides of the jet is negligible. The main parameters governing the jet behaviour are the densimetric Froude number at the outlet, $F_0 = U_0/(gh_0\Delta\rho_0/\rho)^{\frac{1}{2}}$ (expressing the ratio of inertial to buoyancy forces), and the discharge channel aspect ratio, $A = h_0/b_0$. The local Froude number decreases in the downstream direction and also towards the edges of the jet; when it reaches values near unity, buoyancy effects start to dominate and the flow loses its jet character. A subcritical stratified two-layer flow develops in the far field which is governed mainly by the heat loss to the atmosphere and by interfacial friction (in the case of limited size of the receiving water body also by the conditions at the boundaries of this body).

This flow behaves like a spreading warm water pool and is basically an unsteady phenomenon (see the reviews of Jirka, Abraham & Harleman 1975; Dunn, Policastro & Paddock 1975). The transition from the jet-type flow to the stratified flow may occur in form of an internal hydraulic jump. In this paper attention is restricted to the super-critical jet-flow region which depends only on the outlet conditions and which is steady; a procedure is presented for calculating the velocity and the temperature distribution in this region.

1.2. *Previous work*

A number of experimental studies have been carried out to investigate the behaviour of heated surface discharges into stagnant waters, including both laboratory studies and field measurements under full-scale, plant-operating conditions. A brief review is given here on the former which appear to be more suitable for thorough mathematical model verification because they can be performed under better controlled conditions and provide more detailed information†. However, the flow situation introduced above can only be realised to a certain degree in the laboratory because of the limited size of the tank into which the heated water is discharged. In contrast to the real-life situation, heat loss to the surrounding air is insignificant, and prolonged steady conditions can be obtained only when the discharged heat is removed entirely from the tank, e.g. by overflow over a weir, ideally on all sides of the tank. In addition, the water which the jet will entrain has to be specially supplied to the tank (make-up water), and care must be taken that the entrained water is at the ambient temperature. Due to the limited size of the tank and the possibility of incomplete heat removal there is a danger of recirculation and re-entrainment of heated water. The tank geometry exercises a downstream control on the flow, but only on the subcritical part outside the jet region of interest here. Therefore reliable information on the jet region can be obtained in the laboratory provided the make-up water is supplied in such a way that the jet always entrains water at ambient temperature, and provided the control is such that the jet does not end in a hydraulic jump close to the outlet.

Hayashi & Shuto (1967) were among the first to make detailed temperature measurements in this flow situation. Their tank had however no provisions for heat removal and make-up water supply so that they could not achieve steady state conditions, as is indicated by the large scatter of their temperature data. Stefan & Schiebe (1970) used a tank with an overflow weir as downstream control and supplied make-up water through a horizontal slot located at the tank bottom and underneath the hot-water outlet. No indication is given as to how these controls were set. They present velocity and temperature measurements for exit Froude numbers F_0 of 0·62 and 3·73. In the former case a cold water wedge penetrated into the discharge channel and there was no jet-flow region, whilst in the case of $F_0 = 3{\cdot}73$ an internal hydraulic jump appears to have occurred very close to the outlet. Both cases are therefore not suitable for verification of mathematical jet models. Stolzenbach & Harleman (1971) conducted an experiment in a very wide tank; water was withdrawn at the rear through a manifold beneath the surface and was partly re-supplied as make-up water near the tank bottom along the side walls. The manifold had no selective withdrawal capacity; it therefore

† Readers interested in reviews on field data are referred to Shirazi (1975) and Dunn *et al.* (1975).

seems unlikely that the heat was fully removed from the tank, and some of the heated water probably returned upstream underneath the jet and was re-entrained. It appears that the make-up water, which itself was not necessarily at ambient temperature, mainly created a slow ambient current from the side walls to the rear but was not entrained. The notion that the entrained water was not at ambient temperature explains the plateau in the surface centre-line temperature decay measured by Stolzenbach & Harleman at intermediate distances from the outlet. Such a plateau was not observed in prototype situations (see Dunn *et al.* 1975). Stolzenbach & Harleman covered the Froude-number range $1 < F_0 < 9{\cdot}5$ but performed only temperature measurements and presented mainly the development of surface centre-line temperature and jet half widths and depths. Very detailed information on both the temperature and velocity field is available from the experiments of Pande & Rajaratnam (1975) which cover the range $0{\cdot}94 \leqslant F_0 \leqslant 2{\cdot}56$. These authors removed the heated water by an overflow over adjustable tailgates at the downstream end of the tank and supplied make-up water through holes in pipes running along the floor of the tank. The amount of make-up water was determined in preliminary experiments to establish steady state conditions. Because there is only vertical entrainment in the flow considered, this method of make-up water supply from the tank floor seems most suitable to ensure that it is the make-up water at ambient temperature which is actually entrained. For this reason, but also because they are the most comprehensive, Pande & Rajaratnam's measurements seem best suited for a thorough validation of mathematical models. One disadvantage of their particular set-up was the relatively small width of their tank which, at low Froude numbers, may have led to some interference between jet and side walls in the downstream region. The most recent data are due to Wiuff (1978) who used a weir overflow at the rear of his tank but did not supply any make-up water, his flow conditions were therefore only quasi-steady. He reports on an internal wave front moving through the tank; this wave is reflected at the back end, but all the measurements were taken in the supercritical regime before the reflected wave arrived. Wiuff measured the velocity and temperature distribution only at the surface and only for one Froude number (3.6).

All the experiments agree qualitatively on the strong lateral spreading and the small or even absent vertical spreading of the jet. One further feature observed in most experiments is that, in the lateral direction, the excess temperature does not go to zero at the jet edge, so that a stratification is set up outside the jet; the jet edge is defined here as the locus of zero longitudinal velocity. Stefan & Schiebe (1970) argue that the establishment of ambient stratification in their experiment is due to an influence of the downstream control transmitted upstream by virtue of internal gravity. Another explanation would be that heat is simply convected outward by the lateral velocity (buoyant spreading) beyond the jet edge. This notion is supported by Wiuff's (1978) data which indicate significant outward lateral velocities at the jet edge. Further, ambient stratification was present in this study even though the gravity wave front reflected at the downstream end had not yet arrived so that no downstream influence was present.

A short review on existing mathematical models for the surface discharge problem considered here will now be given (more detailed reviews can be found in Dunn *et al.* (1975) and Jirka *et al.* (1975)). The models can be placed into two broad categories, here referred to as integral methods and numerical methods. Integral methods (e.g.

Stolzenbach & Harleman 1971) use profile assumptions for the velocity and temperature distributions in the lateral and vertical directions which allow the governing partial differential equations to be integrated over the jet cross section to yield ordinary differential equations. To close the resulting set of equations, additional assumptions are necessary on the entrainment into the jet and its dependence on buoyancy, as well as on the lateral jet spreading or alternatively the lateral velocity. Integral methods are simple and economic, but many of the assumptions involved do not have a sound physical basis and some are simply incorrect. For example, Stolzenbach & Harleman assume a lateral velocity profile which goes to zero at the jet edge; this is contrary to physical reasoning and to experimental evidence (Pande & Rajaratnam 1975; Wiuff 1978). Further, all integral methods include lateral entrainment, which in reality is negligible at the low Froude numbers of interest. Some models specify this entrainment directly, other methods calculate the lateral spreading as the sum of buoyant and non-buoyant spreading, whereas in fact the lateral spreading is entirely due to buoyancy. The assumption of similarity profiles itself is not entirely realistic (Wiuff 1978) and makes it difficult to cope with the initial development region. Based on extensive test calculations, Dunn *et al.* (1975) conclude that the performance of integral methods is generally disappointing. Furthermore, the extension of these methods to account for other effects like bottom interference, ambient stratification, wind stress, boundary interference or unsteadiness is very problematic because of the weak physical foundation, and it is often difficult if not impossible.

Recently Engelund (1976) proposed an analytical model which is physically more sound. He assumed the profiles to be similar only in the vertical direction and determined the lateral profiles from the equations integrated over the jet depth using a perturbation technique; he correctly retained only inertial and buoyancy terms in the momentum equations. Engelund's model describes Wiuff's (1978) data fairly well, but lacks other verification. It is also difficult to extend for inclusion of other effects as mentioned above.

A model similar to Engelund's, but of the finite-difference type (it therefore falls really into neither integral nor numerical category) is that of Demuren & Spalding (1977). They assume the vertical profiles within the jet are uniform and thus obtain a set of two-dimensional equations for the two velocities U and V, temperature T and the local jet-depth h (termed 'layer-thickness'). As in other models discussed so far an entrainment function must be specified and the data of Chu & Vanvari (1976) and Ellison & Turner (1959) were used. The model certainly possesses many promising features including for example the economic advantage which a two-dimensional model brings, and the ability to be extended to jets in cross-flow. Up to now however, it has only been tested against the rather suspect data of Stolzenbach & Harleman (1971), and the assumption of uniform profiles in the vertical direction may in some cases be too crude (it does not accord with experimental measurements, see figure 7).

The other group of models, usually labelled 'numerical', solve the governing partial differential equations directly, using finite-difference or finite-element techniques. The models of Waldrop & Farmer (1974) and of Paul (1973) are typical examples. These models do not require profile and spreading assumptions and are therefore much more flexible; buoyancy enters these models naturally through exact terms in the equations. An assumption is however necessary about the turbulent transport terms appearing

in the momentum and temperature equations. The existing models use very crude assumptions such as uniform eddy viscosities/diffusivities, empirically modified for the effect of buoyancy. Furthermore, these models have usually solved the full three-dimensional elliptic partial differential equations without simplification, resulting in large computer storage requirements and long computing times. Hence, these methods are very expensive to use. Dunn *et al.* (1975) found their test applications of various numerical models to surface discharge problems somewhat inconclusive but state that these models are promising, especially when the turbulence representation can be improved and the computer storage and time requirements reduced.

1.3. *Present contribution*

The foregoing has shown that the available models are not entirely satisfactory; some lack flexibility and physical soundness (integral methods), others are very expensive and use inadequate turbulence assumptions (numerical methods). In this paper a model is introduced which is intended to fill the existing gap; it is a numerical model and therefore does not require assumptions about profiles and lateral spreading. However, in contrast to existing numerical models, it does not solve the full elliptic equations but the simpler parabolic equations suitable for jet-type problems which were also the starting point for the integral methods. This simplification enables the use of a much more economic numerical solution technique. In addition, the simplistic treatment of turbulence is replaced by a more refined turbulence model, which is a buoyancy-extended version of the widely tested $k-\epsilon$ model (see, e.g. Launder & Spalding 1974; Rodi 1978) employing two extra differential equations for turbulence properties. The effects of buoyancy on the turbulence arise naturally in the exact equations for turbulence properties from which the modelled equations are derived.

The new mathematical model has already been described briefly in McGuirk & Rodi (1977) where it was also tested against the data of Stolzenbach & Harleman (1971) and Hayashi & Shuto (1967), which, as discussed above, now appear not very suitable for comparison purposes. In a further paper McGuirk & Rodi (1979) have shown that a non-buoyant version of the model describes well the limiting case of a three-dimensional isothermal free jet. In the present paper attention is restricted to surface discharges with relatively low Froude numbers (say in the range $1 < F_0 < 5$), and the form of the model suitable for this problem is described in detail in § 2. In § 3 the model is applied to three experimental situations studied by Pande & Rajaratnam (1975) and is compared with their data which appear to be most suitable for verification purposes; the calculated results are further examined and discussed in § 4. The final section of the paper summarizes the model performance and discusses the possibilities of extending the model which, in its present form, is suitable only for discharges into deep, stagnant lakes.

2. Mathematical model

2.1. *Mean flow equations*

The equations governing the velocity and temperature distribution in three-dimensional heated surface jets with significant buoyancy effects may be written as follows

$$\frac{\partial U}{\partial x}+\frac{\partial V}{\partial y}+\frac{\partial W}{\partial z}=0, \tag{1}$$

$$\frac{\partial U^2}{\partial x}+\frac{\partial UV}{\partial y}+\frac{\partial UW}{\partial z}=-\frac{\partial}{\partial x}\int_{-\infty}^{z}\frac{\Delta\rho}{\rho}g\,dz-\frac{\partial\overline{uw}}{\partial z}, \tag{2}$$

$$\frac{\partial UV}{\partial x}+\frac{\partial V^2}{\partial y}+\frac{\partial VW}{\partial z}=-\frac{\partial}{\partial y}\int_{-\infty}^{z}\frac{\Delta\rho}{\rho}g\,dz-\frac{\partial\overline{vw}}{\partial z}, \tag{3}$$

$$\frac{\partial UT}{\partial x}+\frac{\partial VT}{\partial y}+\frac{\partial WT}{\partial z}=-\frac{\partial\overline{wT'}}{\partial z}, \tag{4}$$

$$\rho=f(T), \tag{5}$$

where (1) is the continuity equation, (2) and (3) are momentum equations in the x and y directions respectively (the Boussinesq approximation has been invoked), (4) is the thermal energy equation and (5) is the equation of state for water (see, e.g. Batchelor 1967). The symbols are defined in figure 1.

Equations (1) to (5) form a closed set, when the turbulent shear stresses $\overline{uw}$ and $\overline{vw}$ and the turbulent heat flux $\overline{wT'}$ are specified. Equations (2) to (4) are reduced forms of the general three-dimensional elliptic equations as simplified by Stolzenbach & Harleman (1971) using order of magnitude arguments. A brief account of these arguments will now be given. One basic assumption is that vertical acceleration is small, so that the vertical momentum equation can be reduced to the hydrostatic pressure relation

$$P=-\int_{\eta}^{z}\rho g\,dz,$$

where η is the elevation of the water surface. Preliminary calculations by the authors without using the hydrostatic pressure assumption (i.e. solving also the full vertical momentum equation) have shown that this assumption is indeed reasonable for the heated surface jet problem. With the hydrostatic pressure relation, the pressure gradients $\partial P/\partial x_i$ appearing in the x and y momentum equations ($x_i=x,y$) can be expressed as

$$-\frac{\partial P}{\partial x_i}=-g\rho\frac{\partial\eta}{\partial x_i}-\frac{\partial}{\partial x_i}\int_{\eta}^{z}g\Delta\rho\,dz,$$

where $\Delta\rho$ is the difference between local and ambient density. The surface slope term can be eliminated via the assumption that there should be no horizontal motion and thus no $\partial P/\partial x_i$ at large depths ($z\to-\infty$). Accordingly, the pressure gradient terms can be expressed by the density–difference terms shown in equations (2) and (3).

A second simplification concerns the turbulent shear stress and heat flux terms appearing in the original momentum and thermal energy equations. Because the flow extends much farther in the longitudinal and lateral directions than in the vertical,

gradients in the latter are much larger than in the former two; as a consequence turbulent transport is important only in the vertical direction. Accordingly, turbulent momentum and heat fluxes in the longitudinal and lateral directions have been neglected. The neglect of the longitudinal fluxes is in accord with the usual boundary layer approximation for jet-type flows, while the neglect of lateral fluxes is permissible only for strongly buoyant surface jets. The omission of these flux terms from the equations makes the originally elliptic equations parabolic in both the longitudinal and lateral direction *if*, in addition, the density difference terms (pressure gradient) are assumed known. As will be discussed shortly, this change in equation type is essential for an economic solution of the equations. In physical terms, the parabolic nature implies that influences can be transmitted only in the directions of positive velocities, that is here in the directions of increasing x and y.

2.2. *Turbulence model*

Equations (1) to (5) can be solved to determine the velocity and temperature distribution only when the turbulent shear stresses $\overline{uw}$ and $\overline{vw}$ and the vertical heat flux $\overline{wT'}$ are specified with the aid of a turbulence model. An important aspect of the present flow situation is the influence of buoyancy on the turbulence; we therefore choose as starting point for the development of a suitable turbulence model the exact transport equations for the turbulent stresses and heat fluxes in which buoyancy terms appear as a natural outcome of their derivation from the Navier–Stokes equations. To obtain a closed set of equations, model assumptions have to be introduced for certain terms in the exact equations, not however for the buoyancy terms. With the model assumptions of Launder (1975, 1976) and Launder, Reece & Rodi (1975), the transport equations can be written in tensor form as

$$\underbrace{U_l\frac{\partial\overline{u_iu_j}}{\partial x_l}}_{\text{convective transport}} = \underbrace{c_s\frac{\partial}{\partial x_l}\left(\frac{k}{\epsilon}\overline{u_ku_l}\frac{\partial\overline{u_iu_j}}{\partial x_k}\right)}_{\text{turbulent diffusive transport}} \underbrace{-\overline{u_iu_l}\frac{\partial U_j}{\partial x_l}-\overline{u_ju_l}\frac{\partial U_i}{\partial x_l}-\beta(g_i\overline{u_jT'}+g_j\overline{u_iT'})}_{P_{ij}\text{: stress production, buoyancy production}}$$

$$\underbrace{-c_1\frac{\epsilon}{k}(\overline{u_iu_j}-\tfrac{2}{3}\delta_{ij}k)}_{\text{pressure-strain}} - \underbrace{c_2(P_{ij}-\tfrac{2}{3}\delta_{ij}P)}_{\text{pressure-strain}} - \underbrace{\tfrac{2}{3}\epsilon\delta_{ij}}_{\text{viscous dissipation}}, \qquad (6)\dagger$$

$$\underbrace{U_l\frac{\partial\overline{u_iT'}}{\partial x_l}}_{\text{convective transport}} = \underbrace{c_{s\phi}\frac{\partial}{\partial x_l}\left(\frac{k}{\epsilon}\overline{u_ku_l}\frac{\partial\overline{u_iT'}}{\partial x_k}\right)}_{\text{turbulent diffusive transport}} \underbrace{-\overline{u_iu_j}\frac{\partial T}{\partial x_j}-\overline{u_jT'}\frac{\partial U_i}{\partial x_j}-\beta g_i\overline{T'^2}}_{P_{iT}\text{: mean field production } P_{iT,v},\ \text{buoyancy production}}$$

$$\underbrace{-c_{1T}\frac{\epsilon}{\kappa}\overline{u_iT}}_{\text{pressure-temperature-gradient correlation}} - c_{2T}P_{iT,v}. \qquad (7)$$

† $\overline{u_iu_j}$ is the transport of x_j momentum in x_i direction and $\overline{u_iT'}$ the transport of heat in x_i direction.

The physical meaning of the individual terms is indicated in the equations. The terms representing diffusion, pressure–strain and pressure–temperature correlations, as well as dissipation are model approximations and therefore contain various empirical constants c†; the other terms are exact. The contraction of the $\overline{u_i u_j}$ equation (6) yields the equation for the turbulent kinetic energy k, in which P appears as the total production (stress and buoyancy) and ϵ as the dissipation of k. Since the fluctuating temperature $\overline{T'^2}$ appears as a buoyancy production term in the $\overline{u_i T'}$ equation, it is necessary to add the transport equation for this quantity, which reads

$$U_l \frac{\partial \overline{T'^2}}{\partial x_l} = c_{sT} \frac{\partial}{\partial x_l}\left(\frac{k}{\epsilon}\overline{u_k u_l}\frac{\partial \overline{T'^2}}{\partial x_k}\right) - 2\overline{u_l T'}\frac{\partial T}{\partial x_l} - \frac{\overline{T'^2}}{kc_T}\epsilon. \tag{8}$$

convective transport; turbulent diffusive transport; production; viscous destruction

In this equation, the diffusion and dissipation terms are model approximations due to Launder (1975, 1976).

The determination of turbulent stresses and heat fluxes by means of equations (6) to (8) or similar model equations is usually referred to as 'second-order closure' and is conceptually the most realistic method of simulating turbulent transport processes at the present state of development. However, this type of modelling requires the solution of a fairly large number of additional differential equations, which makes it computationally very expensive, especially for complex flow situations such as the one considered here. Hence, the above equations are used here merely as a starting point for the derivation of a simpler model. When, as suggested by Launder (1975), the convective and diffusive transport terms are neglected in the above equations, these reduce to the following algebraic expressions:

$$\frac{\overline{u_i u_j}}{k} = \frac{P_{ij}}{\epsilon}\frac{1-c_2}{c_1} - \tfrac{2}{3}\delta_{ij}\frac{1-c_1-c_2}{c_1}, \tag{9}$$

$$\overline{u_i T'} = \frac{k}{c_{1T}\epsilon}(P_{iT} - c_{2T}P_{iT,v}), \tag{10}$$

$$\overline{T'^2} = -\frac{2}{c_T}\frac{k}{\epsilon}\overline{u_l T'}\frac{\partial T}{\partial x_l}. \tag{11}$$

The neglect of convection and diffusion terms implies the assumption that turbulence is near a state of local equilibrium. It is consistent with this assumption that, in the expression for the normal stresses ($i = j$), the turbulent kinetic energy production P appearing in (6) is set equal to the dissipation ϵ. It is important to note that the direct buoyancy influence is retained in (9) and (10) *via* the production terms.

For the present flow situation it is assumed that the only significant gradients are $\partial U/\partial z$, $\partial V/\partial z$ and $\partial T/\partial z$. The only gravitational component is $g_3 = -g$ (where $x_3 = z$ is vertically upward). Equations (9) to (11) then yield for the quantities relevant to this problem:

$$\frac{\overline{w^2}}{k} = \frac{(1-c_2)}{c_1\epsilon}(2\beta g\overline{wT'}) - \frac{2}{3}\frac{(1-c_1-c_2)}{c_1}; \tag{12}$$

† The dissipation term is based on the assumption of local isotropy which does not introduce an empirical constant. Owing to the same assumption the dissipation term originally present in the $\overline{u_i T'}$ equation vanishes.

$$\frac{\overline{uw}}{k} = \frac{(1-c_2)}{c_1\epsilon}\left(-\overline{w^2}\frac{\partial U}{\partial z} + \beta g\overline{uT'}\right); \tag{13}$$

$$\frac{\overline{vw}}{k} = \frac{(1-c_2)}{c_1\epsilon}\left(-\overline{w^2}\frac{\partial V}{\partial z} + \beta g\overline{vT'}\right); \tag{14}$$

$$\overline{uT'} = \frac{k}{c_{1T}\epsilon}\left(-\overline{uw}\frac{\partial T}{\partial z} - \overline{wT'}\frac{\partial U}{\partial z} + c_{2T}\overline{wT'}\frac{\partial U}{\partial z}\right); \tag{15}$$

$$\overline{vT'} = \frac{k}{c_{1T}\epsilon}\left(-\overline{vw}\frac{\partial T}{\partial z} - \overline{wT'}\frac{\partial V}{\partial z} + c_{2T}\overline{wT'}\frac{\partial V}{\partial z}\right); \tag{16}$$

$$\overline{wT'} = \frac{k}{c_{1T}\epsilon}\left(-\overline{w^2}\frac{\partial T}{\partial z} + \beta g\overline{T'^2} - c_{2T}\beta g\overline{T'^2}\right); \tag{17}$$

$$\overline{T'^2} = -\frac{2}{c_T}\frac{k}{\epsilon}\overline{wT'}\frac{\partial T}{\partial z}. \tag{18}$$

These expressions can be rearranged to yield explicit formulae† for $\overline{uw}$, $\overline{vw}$ and $\overline{wT'}$ in terms of velocity and temperature gradients k, and ϵ; these relations may then be written in a form similar to the Kolmogorov–Prandtl eddy viscosity/diffusivity formulae, namely:

$$-\rho\overline{uw} = \mu_t\frac{\partial U}{\partial z}, \quad -\rho\overline{vw} = \mu_t\frac{\partial V}{\partial z}, \quad -\rho\overline{wT'} = \frac{\mu_t}{\sigma_t}\frac{\partial T}{\partial z} \quad \text{with} \quad \mu_t = \rho c_\mu\frac{k^2}{\epsilon}. \tag{19}$$

The parameter c_μ and the turbulent Prandtl number σ_t, usually assumed constant, are now functions of the buoyancy as specified by (12) to (18). The temperature dependance of volumetric expansion coefficient β appearing in the buoyancy terms is obtained from the literature (Batchelor 1967).

Equations (12) to (18) contain the turbulence parameters k and ϵ, which are still unknown. The procedure adopted here to determine k and ϵ is to solve extra differential transport equations for these quantities; these equations have been used as part of the so-called $k-\epsilon$ turbulence model in many non-buoyant flow calculations (Launder & Spalding 1974; Rodi 1978). Here, the following equations suitable for horizontal buoyant flows are employed:

$$\frac{\partial Uk}{\partial x} + \frac{\partial Vk}{\partial y} + \frac{\partial Wk}{\partial z} = \frac{\partial}{\partial z}\left(\frac{\mu_t}{\rho\sigma_k}\frac{\partial k}{\partial z}\right) - \overline{uw}\frac{\partial U}{\partial z} - \overline{vw}\frac{\partial V}{\partial z} + \beta g\overline{wT'} - \epsilon, \tag{20}$$

$$\frac{\partial U\epsilon}{\partial x} + \frac{\partial V\epsilon}{\partial y} + \frac{\partial W\epsilon}{\partial z} = \frac{\partial}{\partial z}\left(\frac{\mu_t}{\rho\sigma_\epsilon}\frac{\partial \epsilon}{\partial z}\right) - c_{\epsilon 1}\frac{\epsilon}{k}\left(\overline{uw}\frac{\partial U}{\partial z} + \overline{vw}\frac{\partial V}{\partial z}\right) - c_{\epsilon 2}\frac{\epsilon^2}{k}. \tag{21}$$

The k equation (20) can be obtained by contraction of the $\overline{u_i u_j}$ equation (6) and by retaining only the significant gradients with respect to z. Hossain & Rodi (1977) have investigated the nature of the buoyancy term in this equation; they have shown that the heat flux $\overline{wT'}$ is negative in the heated surface jet so that the buoyancy term acts to reduce turbulence energy and, as a consequence, also the eddy viscosity and the ability of the jet to entrain ambient fluid. Hossain & Rodi (1977) have also found that, in contrast to the situation in vertical buoyant jets, there should be no corresponding

† The formulae are rather cumbersome and are therefore not included here.

c_1	c_2	$c_{\epsilon 1}$	$c_{\epsilon 2}$	σ_k	σ_ϵ	c_{1T}	c_{2T}	c_T
2·2	0·55	1·44	1·92	1·0	1·3	3·2	0·5	1·25

TABLE 1. Constants in the turbulence model

buoyancy term in the ϵ equation. This finding is supported also by Gibson & Launder's (1976) two-dimensional heated surface jet calculations.

The turbulence model equations (12) to (21) complement the mean-flow equations (1) to (5) to form a closed set; before this can be solved, the 9 empirical constants of the model must be specified. Here we simply adopt values suggested in the literature. The constants c_1 and c_2 appear in the pressure-strain term of the $\overline{u_i u_j}$ equation (6), the constants $c_{\epsilon 1}$ and $c_{\epsilon 2}$ in the source/sink terms of the ϵ equation (21) and σ_k and σ_ϵ in the diffusion terms of the k and ϵ equations; they were all determined by reference to experiments in simple non-buoyant flows (Launder & Spalding 1974; Launder *et al.* 1975). The remaining 3 constants appearing in the heat-flux and $\overline{T'^2}$ equations were determined by Launder (1975) from experiments on turbulence subjected to uniform velocity and temperature gradients and on the decay of temperature fluctuations behind a heated grid. The values of all the constants are given in table 1. It should be stressed here that none of the constants have been adjusted to suit the present problem; they are all unchanged from those quoted in the literature, where they were determined by reference to experiments on much simpler flows.

2.3. *Solution procedure*

The equations (4), (20) and (21) are parabolic in the x and y directions because no second derivatives appear with respect to these directions; if the pressure gradients arising from density differences are considered as known, the momentum equations (2) and (3) are also parabolic. All these equations can therefore be solved with the general solution procedure for three-dimensional parabolic equations developed by Patankar & Spalding (1972). Indeed, an even more complex equation set could be treated with this method where the pressure field was also unknown, a third momentum equation had to be solved, and the equations were parabolic only in one direction (main flow direction). The solution procedure has been simplified for the present work as the steps in the procedure necessary to establish the pressure field and to solve the third momen tum equation are redundant for the present problem. The finite-difference formulation is however exactly as in the original work, and hence no details need to be given here; merely the main steps in the solution procedure are now outlined.

The solution is obtained by a marching integration in the downstream direction (x), starting from known values of all the dependent variables at the discharge cross-section. This manner of integration can be adopted since the equations are parabolic in the x direction; it is particularly economic because, in contrast to solution procedures for three-dimensional elliptic equations, it needs only two-dimensional storage and does not require iteration. Further, the dependent variables are stored at the nodes of a finite-difference grid which just covers the area of interest, namely the jet area: at the inlet, the grid only covers the discharge area, but it expands with downstream distance

as the jet spreads. A forward integration step, in which the unknown values of the variables at a downstream plane are determined, is carried out as follows:

(1) The U and V momentum equations are solved first, using known upstream values of density in the pressure-gradient terms; for the gradient $\partial\Delta\rho/\partial y$ only values at the immediate upstream plane are taken while the gradient $\partial\Delta\rho/\partial x$ is determined by extrapolation from the 2 preceding upstream planes. Some upstream values are also used for calculating the shear stresses $\overline{uw}$ and $\overline{vw}$.

(2) The continuity equation is solved next to obtain the W velocity field.

(3) The differential equations for scalar properties are then solved in the order T, k, ϵ, at each stage using the latest available values to calculate the shear stresses and the heat flux.

The solution has now been established for all variables at the downstream plane; this process is then repeated for as many steps in the x direction as are necessary to cover the region of interest. Step sizes are small near the discharge (typically one-tenth of 1 % of the jet depth) and are increased to about 20 % of the jet depth further downstream. The effect of step size has been tested to ensure that the solution is step-size independent, as has the number of grid nodes used in each direction; a 16×16 grid appears to be sufficiently fine. Typical computing times and core-storage requirements for a single run are 7 minutes and 30 K words on a UNIVAC 1108 machine.

In order to be able to distribute the finite-difference grid over only the jet region, it is necessary to allow the grid cross-section to change its vertical and horizontal dimensions with downstream distance. A method for accomplishing this within the present solution procedure has been developed by Sharma (1974) for flows in ducts of axially-varying cross-section; the method requires only that the changes in dimensions of the grid be specified in any forward step; how this has been done is now described.

In the integral solution procedure derived by Stefan & Vaidyaraman (1972), equations were derived for the horizontal and vertical spreading of a buoyant surface jet by analogy with the unsteady buoyant spread of a pool of warm water floating on stagnant cold water. In the present work these formulae are also used but merely to prescribe the spread of the grid and not the jet itself, although modified as shown below by the use of two factors f_1 and f_2

$$\frac{db_G}{dx} = f_1 \frac{a_1}{F_{\mathbb{Q}}}, \tag{22}$$

$$\frac{dh_G}{dx} = a_2 - f_2 \frac{h_G}{b_G} \frac{a_1}{F_{\mathbb{Q}}}. \tag{23}$$

In equations (22) and (23) b_G and h_G stand for the total grid width and grid depth respectively. The terms involving the f-factors account for the buoyant spreading, with a_1 being a coefficient for which Stefan gave the value 0·66; the same value is retained here. In the expression for the vertical spread, a_2 allows for spreading due to entrainment and has been given a value of 0·22; this value is however reduced proportionally as the effective viscosity at the jet bottom is reduced by buoyancy.

The use of such equations has been criticised by Jirka *et al.* (1975) and by Dunn *et al.* (1975) as having an insecure theoretical base; the justification for their employment here is that they are used only to ensure that the boundaries of the grid are outside the jet region, but not so far outside that many grid points are wasted in the ambient

region. As the equations are parabolic in the lateral direction, the conditions at the side edges of the grid do not influence the calculated jet properties so that the choice of the grid width does not affect the calculations. On the other hand, the conditions at the bottom edge of the grid do have an influence so that care has to be taken that this grid boundary lies in the ambient region. To ensure that the grid control formulae did not affect the calculations, the factors f_1 and f_2 were introduced and varied until they had no influence on the results other than to place the jet boundaries further into the ambient fluid; values of between 2 and 4 were used for f_1 and between 0·5 and 3 for f_2. Other spreading formulae have been proposed in the literature (e.g. Shirazi & Davis 1976) which may be improvements on the formulae used here, but they would not lead to different predictions.

The finite-difference equations are derived in a co-ordinate system aligned with the numerical grid. This system is assumed to be quasi-orthogonal so that strictly the spreading angle of the grid should be small, say not more than about 20°. In the present work the lateral jet spreading and consequently the grid spreading is significantly larger than this, so that certain numerical errors are introduced near the jet edge. However, these errors appear to have little overall influence on the calculations because they occur in the relatively unimportant edge region. This is confirmed by the overall conservation of momentum

$$\int_A (\rho U^2 + B)\, dA = \text{const.}, \quad \text{where} \quad B = \int_{-\infty}^{z} \Delta\rho\, g dz$$

and heat

$$\int_A (\rho \Delta T U)\, dA = \text{const.},$$

which was checked at various cross sections and never found to change by more than -5% (this figure includes heat outflow at the jet edge).

2.4. *Initial and boundary conditions*

It has been mentioned above that initial distributions of all variables are required; boundary conditions must also be prescribed for all variables at the free surface, the bottom edge of the grid and at the vertical centre plane; as the equations are parabolic in the lateral direction and the side edge of the jet forms an outflow boundary, no conditions need to be specified there. The finite-difference grid cross-section at any plane may be depicted as shown in figure 2 on which all the boundary conditions used are shown. The heat transfer at the water surface is prescribed using a heat transfer coefficient K, here given a value $6{\cdot}1 \times 10^{-6}$ m s^{-1} taken from Stolzenbach & Harleman (1971); the calculations with and without surface heat loss however revealed an insignificant influence of this boundary condition. At the inlet it is possible to specify distributions if all variables of these have been measured; this is unfortunately not normally the case and recourse has to be made to some idealisation. In the present case all variables have been specified as uniform at inlet (zero for the lateral velocities V and W) except for the axial velocity; since the jet flow in experiments usually is led along an open channel before discharge, it seemed reasonable to assume that boundary layers would have grown on the channel sides and bottom. Accordingly a boundary layer thickness was chosen and the velocities at all grid points were specified from a one-seventh power law distribution which had the same average velocity as measured

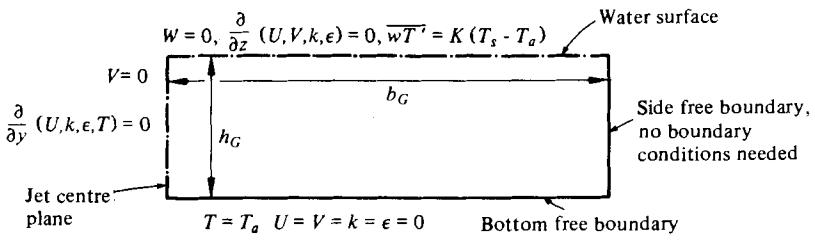

FIGURE 2. Boundary conditions.

Run no. in expts.	A	F_0
1	0·94	2·56
2	0·94	1·67
3	0·316	1·32

TABLE 2. Experimental situations simulated (Pande & Rajaratnam 1975)

in the experiments; the effects of different boundary layer thickness were investigated in a previous paper (McGuirk & Rodi 1977) and were found to be small; here a thickness $\delta/h_0 = 0{\cdot}25$ was used.

For the turbulence quantities, the values within the boundary layer can be calculated from (see Launder & Spalding 1974).

$$k = U_*^2/c_\mu^{\frac{1}{2}}, \quad \epsilon = U_*^3/\kappa l,$$

where U_* is a friction velocity which can be calculated using standard formulae, l is a length scale proportional to δ, the boundary layer thickness, and c_μ and κ are constants (0·09 and 0·42 respectively); in the present calculations the above equations have been used to fix the values of k and ϵ over the whole jet area at inlet.

3. Performance of the model

In a previous paper (McGuirk & Rodi 1977) we have shown that the buoyancy extended turbulence model described in the last section correctly predicts the reduction of entrainment due to buoyancy in the case of the two-dimensional heated surface jet measured by Ellison & Turner (1959). It can therefore be expected that the buoyancy effect on the vertical turbulent exchange processes is also simulated well in the three-dimensional situation considered here. The previous paper also reports on some preliminary testing of the present mathematical model against the data of Stolzenbach & Harleman (1971) and Hayashi & Shuto (1967). The predicted depth and width development of the surface jet agreed fairly well with these measurements, but the agreement on the temperature decay was less satisfactory; in particular, the temperature plateau observed by Stolzenbach & Harleman was not predicted. As was discussed in §1.2, both the experiments of these authors and of Hayashi & Shuto did not correspond closely to a discharge into infinitely large surroundings as assumed in the model; the disagreement is therefore not particularly surprising. In §1.2 the experiments of Pande & Rajaratnam (1975) were found to be more suitable for verification;

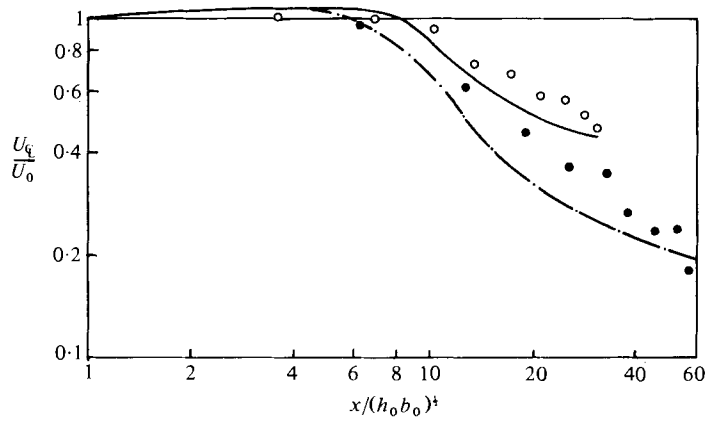

FIGURE 3. Surface centre-line velocity decay. Experimental results (Pande & Rajaratnam 1975): ●, run 1; ○, run 3. Predicted results: —·—, run 1; ——, run 3.

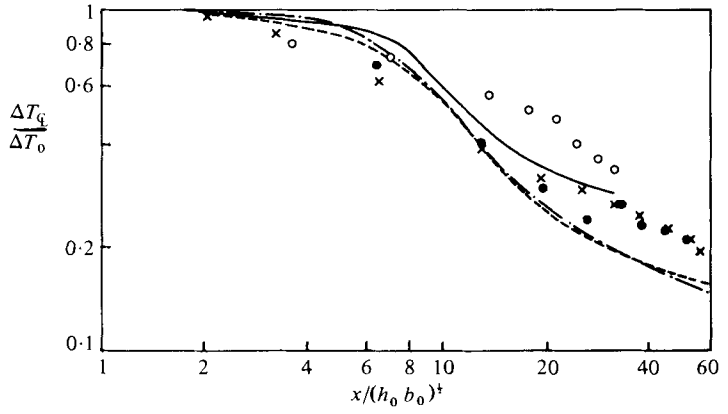

FIGURE 4. Surface centre-line excess temperature decay. Experimental results (Pande & Rajaratnam 1975): ●, run 1; ×, run 2; ○, run 3. Predicted results: —· —, run 1; – – –, run 2; ——, run 3.

in the following the performance of the model is tested against these data. Three experimental situations were selected, for which the aspect ratio A and outlet Froude number F_0 are given in table 2.

3.1. *Decay of centre-line values and jet spreading*

Figure 3 compares predicted and measured decay of centre-line surface velocity (for runs 1 and 3 only). The agreement is generally good; in particular the trend is predicted correctly that the velocity decays slower and levels off sooner for the lower F_0 case (run 3); the former is due to the buoyancy induced, longitudinal pressure gradient (which in fact accelerates the flow slightly at first) and the latter due to the reduction of entrainment due to buoyancy.

The excess temperature decay curves are compared in figure 4. The general agreement is also satisfactory even though the decay is overpredicted somewhat in the downstream region; there the measurements are believed to be less reliable because of the possible interference of the side walls of the tank with the very fast spreading jet.

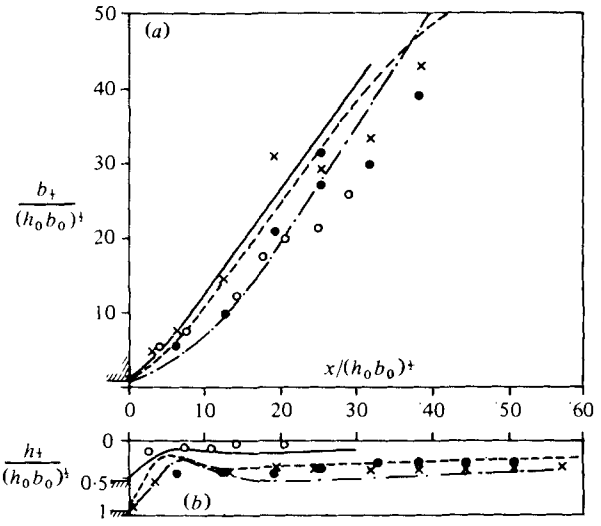

FIGURE 5. Development of half width $b_{\frac{1}{2}}$ (*a*) and half depth $h_{\frac{1}{2}}$ (*b*) (the symbols are the same as in figure 4).

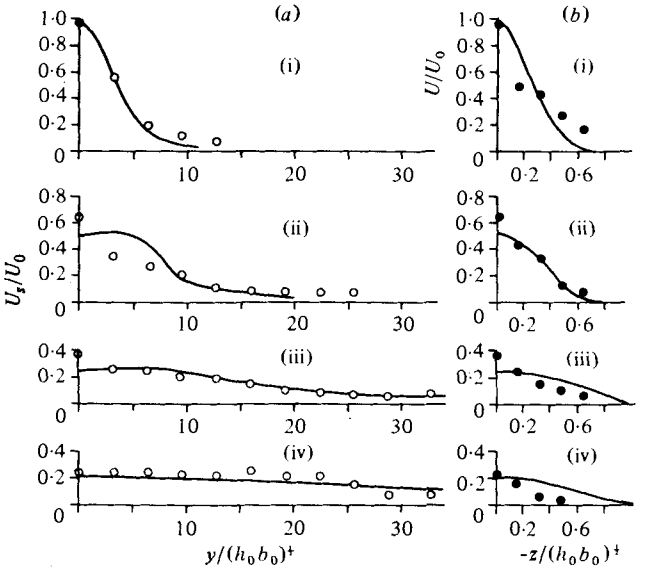

FIGURE 6. Velocity profiles for run 1. (*a*) Horizontal profiles at the surface. (*b*) Vertical profiles at the centre-plane. $x/(h_0 b_0)^{\frac{1}{2}}$ values are: (i) 6·4; (ii) 12·81; (iii) 25·61; (iv) 44·82. ——, predicted; ○, ●, experimental results (Pande & Rajaratnam 1975).

The model predicts correctly that the decay for runs 1 and 2 (same aspect ratio) is essentially the same, but that the decay for the lowest Froude number is slower. The excess temperature can be seen to decay faster than the velocity, which is due to the buoyancy acceleration of the latter mentioned already.

The downstream development of the half width and depth is compared in figure 5. In the initial region the width is very well predicted, including the difference between

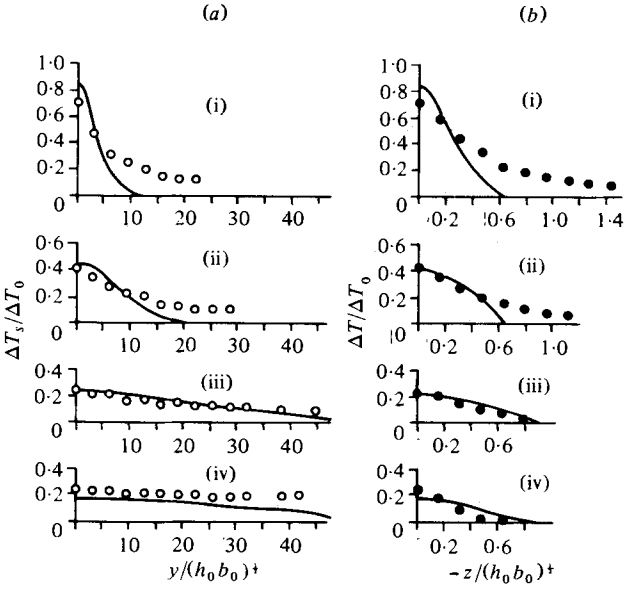

FIGURE 7. Excess temperature profiles for run 1. (*a*) Horizontal profiles at the surface. (*b*) Vertical profiles at the centre-plane. $x/(h_0 b_0)^{\frac{1}{2}}$ values are: (i) 6·4; (ii) 12·8; (iii) 25·6; (iv) 44·8. ——, predicted; ○, ●, experimental results (Pande & Rajaratnam 1975).

run 1 and run 2; in the downstream region the width is somewhat overpredicted, and the disagreement is worst for run 3 with the lowest Froude number. In view of the fact that the spreading is due to buoyancy it appears somewhat strange however that in the experiments the jet with the lowest Froude number should spread least, possibly also a side-wall effect. The half depth behaviour is also generally well predicted, in particular the levelling off to a nearly constant value. The smaller depth for run 2 as compared to run 1 is consistent with the larger lateral spreading but is not borne out by the experiments. The depth for the lowest Froude number case (run 3) is overpredicted. The initial undulations of the half-depth are explained below by looking at the vertical temperature profiles.

3.2. *Profiles and contours*

In this section the ability of the model to describe also the details of the flow behaviour is demonstrated by a few examples of velocity and temperature profile as well as contour plots. For run 1, figure 6 compares predicted and measured lateral surface and vertical centre-plane profiles of longitudinal velocity at various x stations. The agreement can be considered as generally satisfactory even if there is local disagreement. The situation is not quite as good for the corresponding temperature profiles shown in figure 7. Apart from the surface centre-line temperature decaying somewhat too fast in the far field, as seen already in figure 4, the predicted excess temperature approaches zero at the jet edges considerably faster than observed in both lateral and vertical directions in the near field ($x/(h_0 b_0)^{\frac{1}{2}} \leqslant 20$). The relatively large excess temperature observed in the experiment may have been caused by recirculation of heated water; it is difficult to understand how, otherwise, the temperature can be above the ambient temperature at relatively large depths as close to the discharge as

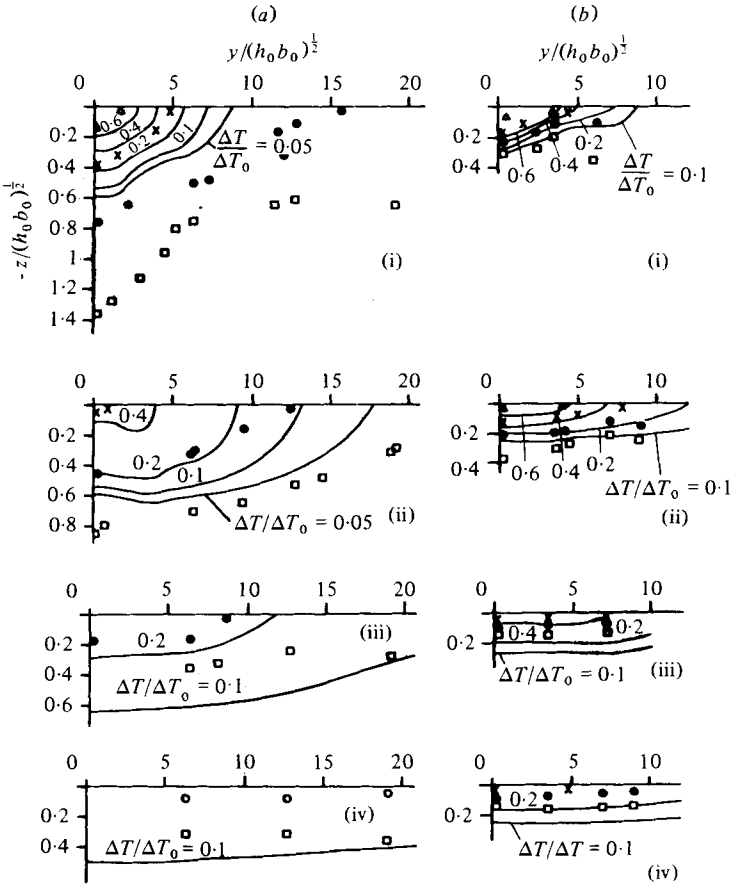

FIGURE 8. Cross-sectional excess temperature contours. (*a*) Run 1, values of $x/(h_0 b_0)^{\frac{1}{2}}$ are: (i) 6·4; (ii) 12·8; (iii) 25·6; (iv) 44·8. (*b*) Run 3, values of $x/(h_0 b_0)^{\frac{1}{2}}$ are: (i) 3·56; (ii) 7·12; (iii) 14·23; (iv) 21·35. Experimental results (Pande & Rajaratnam 1975): △, $\Delta T/\Delta T_0 = 0{\cdot}6$; ×, $\Delta T/\Delta T_0 = 0{\cdot}4$; ●, $\Delta T/\Delta T_0 = 0{\cdot}2$; □, $\Delta T/\Delta T_0 = 0{\cdot}1$. ——, predicted.

$x/(h_0 b_0)^{\frac{1}{2}} = 6$. The possibility of recirculation is supported by Wiuff (1978) who presents a streamline picture obtained by photographing the motion of surface floats. This picture shows clearly that the fast spreading heated surface jet hits the side walls so that part of it is deflected upstream and induces recirculation eddies in the corners formed by the discharge plane and the side walls. As the relative tank width was even smaller in Pande & Rajaratnam's (1975) study, the occurrence of this kind of recirculation was even more likely. The disagreement between predicted and measured lateral profiles at the jet edges may however also be due to the numerical errors in this region mentioned earlier.

Figure 8 presents cross-sectional temperature contours at various axial stations for both experimental runs 1 and 3. These contours show clearly the three-dimensionality of the problem: the cross-sectional jet shape develops from a near-square form at the outlet to a stretched-out surface layer form, and this development is more rapid for the low Froude number case (run 3). The model can be seen to predict well the change in jet shape and its dependence on the Froude number. There is however only limited agree-

ment on the details of the contours; for run 1 the lower excess temperature contours ($\Delta T/\Delta T_0 = 0{\cdot}1$, $0{\cdot}2$) near the discharge extend much further out in the experiment, which may again be explained by recirculation of heated water. The situation is better for run 3 where only the lateral extent is somewhat larger in the experiment while the vertical extent is in agreement with the predictions; this is consistent with the notion that in this case the heated surface jet, and thus also the recirculating water, is contained in a thinner surface layer than in the case of run 1. Further downstream the predicted contours lie outside the measured ones, especially for the low Froude number case 3. This was to be expected from figure 5 which showed that both jet width and depth were overpredicted by the model for runs 1 and 3.

Surface temperature contours are especially suited for obtaining an impression of the water areas contaminated by the heated water discharge. As an example, the surface contours are given for run 1 in figure 1; velocity contours are also included in order to give an idea about the surface velocity field set up by the thermal discharge. As can be seen, the predicted temperature (top) and velocity (bottom) contours both agree fairly well with the measured contours in the near field around the discharge. In the far field the experimental scatter is very large, and there small discrepancies in the actual profiles (see figures 6 and 7) are magnified in the contour plots because of the small profile slopes; the less satisfactory agreement in this area is therefore not surprising. It should also be kept in mind that the present model is applicable only to the jet region of the flow so that from some distance onward reliable predictions cannot be expected in any case. However, the area of applicability cannot be clearly discerned. The surface contours for runs 2 and 3 look similar to those presented in figure 1; the model predicts correctly that the lines of constant velocity and temperature move further out when the Froude number is decreased.

4. Discussion

After the presentation of the main results in the last section, a few aspects of the predictions will now be discussed in greater detail, and some further results will be presented which help to complete our picture of the flow behaviour. First, the undulations of the predicted half depth (see figure 5) are examined. At the discharge the profile is uniform and the half depth is therefore at the bottom of the discharge channel. Two counteracting processes govern the further development of the jet depth: firstly the buoyancy induced upward and lateral motion of the discharged heated water, which reduces the jet depth, and secondly the entrainment of ambient water, which acts to increase the jet depth. Very close to the discharge the upward motion is stronger and overrules the jet spreading due to entrainment so that the depth is reduced. There follows a short region where the spreading dominates the upward motion so that the depth (both half and full) increases again. Further downstream, entrainment has been reduced by buoyancy to such an extent that spreading and upward motion balance each other and the depth remains constant. The intermediate increase in half depth is amplified by a significant change in profile shape, as can be seen from the profiles at $x/(h_0 b_0)^{\frac{1}{2}}$ of $6{\cdot}4$ and $12{\cdot}8$ in figure 7. At the smaller x value the profile has a shape as usually found in jets, while further downstream the profile is much fuller so that the half-depth is a larger proportion of the full depth. This change in profile shape is due to the influence of buoyancy on the turbulence and was obtained also in two-dimensional

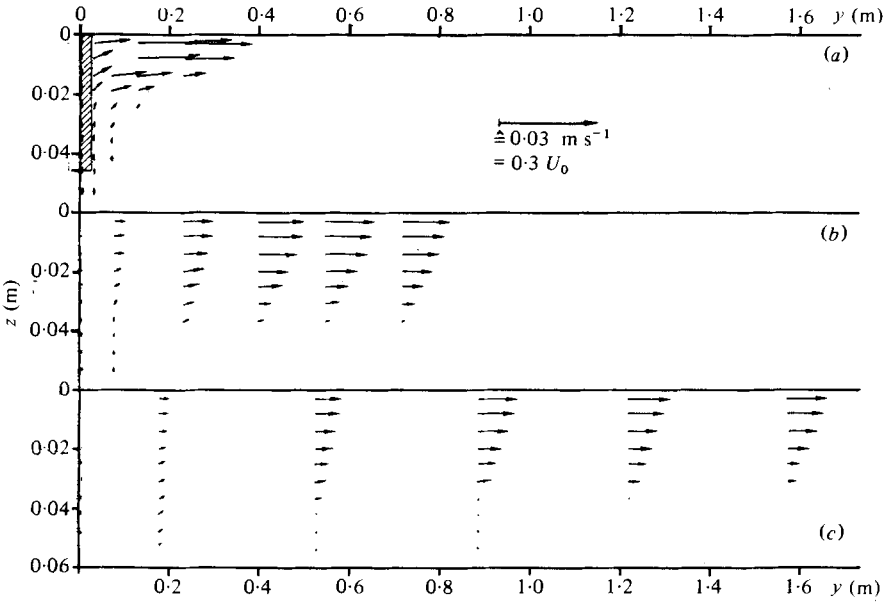

FIGURE 9. Predicted cross-sectional velocity vectors for run 1 (the lateral and vertical scales are different). (*a*) $x/(h_0 b_0)^{\frac{1}{2}} = 6{\cdot}214$. (*b*) $x/(h_0 b_0)^{\frac{1}{2}} = 18{\cdot}5$. (*c*) $x/(h_0 b_0)^{\frac{1}{2}} = 32{\cdot}73$.

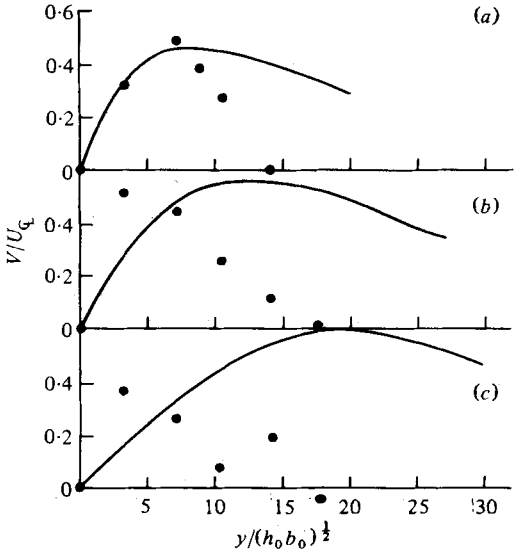

FIGURE 10. Lateral velocity profiles for run 3. (*a*) $x/(h_0 b_0)^{\frac{1}{2}} = 10{\cdot}7$. (*b*) $x/(h_0 b_0)^{\frac{1}{2}} = 14{\cdot}2$. (*c*) $x/(h_0 b_0)^{\frac{1}{2}} = 21{\cdot}3$. ——, predicted; ●, experimental results (Pande & Rajaratnam 1975).

heated surface jet predictions (Hossain 1979). The rather full profile is not however in very good agreement with experimental profiles which nearly follow a straight line (see figure 7 and also Chu & Vanvari 1976 for measurements in a two-dimensional heated surface jet). To obtain better agreement, the turbulence model has to be improved and perhaps more realistic boundary conditions have to be specified at the

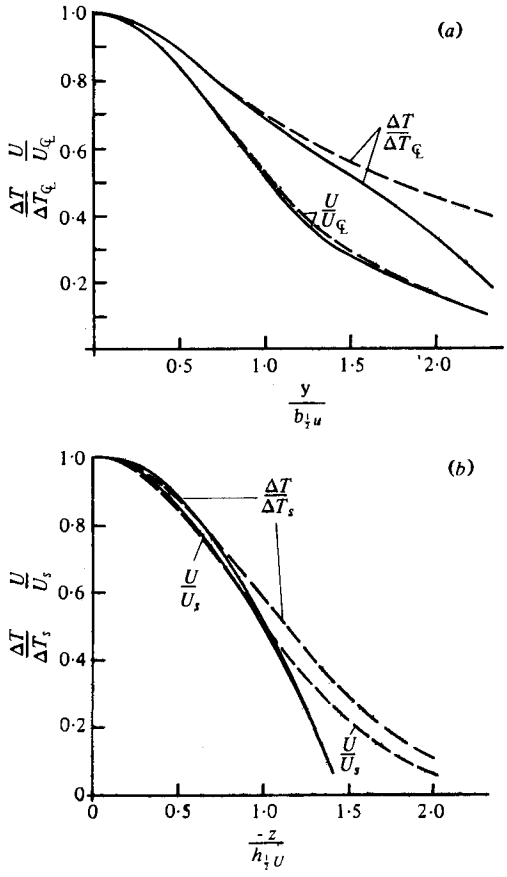

FIGURE 11. Similarity profiles for velocity and excess temperature for run 1 ($22 \leqslant x/(h_0 b_0)^{\frac{1}{2}} \leqslant 40$). (*a*) Horizontal profiles at the surface. (*b*) Vertical profiles at the centre-plane. ——, predicted; ---, experimental results (Pande & Rajaratnam 1975).

free surface. It is mainly due to this discrepancy in profile shape that the predicted half depths show a significant intermediate increase, unlike the measured half-depths.

The buoyancy induced upward and lateral motion can best be illustrated by velocity vector plots as given in figure 9 for three cross sections for the situation of run 1. The shaded area represents the jet at the discharge. The figure illustrates clearly the lateral spreading mechanism by means of relatively large lateral velocities; it also shows that there is no lateral entrainment, as discussed already in the Introduction. The vertical velocities at the lower jet edges are partly buoyancy induced and partly due to entrainment; as can be seen, these velocities have significant values only near the centre plane which also indicates that entrainment takes place mostly in the inner jet region.

The lateral velocity distribution at the surface is compared for run 3 with Pande & Rajaratnam's (1975) measurements in figure 10. The maximum value is roughly in agreement, but near the edge the predicted velocities decrease much more slowly than the measured ones. It seems unreasonable however that the lateral velocity should go to zero at the jet edge (where $U \approx 0$) as indicated by the measurements; according to

the physical picture portrayed in the Introduction the warm water continues to spread outside the jet in the form of a stratified layer. We therefore believe that Pande & Rajaratnam's lateral velocity measurements for run 3† are either unreliable or that the side walls had a serious effect on these velocities which must of course go to zero as the side walls are approached. It is interesting to note that in runs with $F_0 < 1$ Pande & Rajaratnam have measured lateral velocity profiles whose shape agrees with that of the predicted profiles in figure 10. Wiuff (1978) also obtained the same shape in his measurements for $F_0 = 3{\cdot}6$ so that the predicted profiles appear to be close to the truth. Attention should also be drawn to the fact that the lateral velocity reaches the magnitude of the longitudinal velocity roughly at the half width of the jet.

Finally, the shapes of velocity and temperature profiles are compared in figure 11 and will now be discussed. At the surface, vertical diffusion of heat and momentum are zero and, since horizontal diffusion is also negligible, the only difference between the equations governing the lateral distribution of velocity and temperature at the surface is the pressure gradient term

$$\frac{\partial}{\partial x}\int_{-\infty}^{z}\frac{\Delta\rho}{\rho}g\,dz$$

in the longitudinal momentum equation. Omission of this term would lead to identical surface velocity and temperature profiles, as had been shown already by Engelund (1976). The pressure gradient term is accelerative near the centre-line and decelerative at the edge, thus pushing the velocity profile inside the temperature profile, which is in agreement with the measurements. It is important to note that, unlike in non-buoyant submerged jets where heat also spreads faster than momentum, here this fact has nothing to do with turbulent diffusion and the turbulent Prandtl number (ratio of eddy viscosity to diffusivity) being smaller than unity. Turbulent diffusion does however influence the vertical profiles. For these the pressure gradient has the same steepening effect on the velocity profile, but this effect is counteracted by vertical turbulent diffusion. Owing to strong buoyancy effects the turbulent Prandtl number is larger than unity (this is also predicted by the turbulence model) which would lead to a velocity profile outside the temperature profile. The counter effect of the pressure gradient causes the two profiles to lie very close together, which is borne out by both predictions and experiments. The pressure gradient term in the momentum equation gains importance as the Froude number decreases, and it should be mentioned here again that this term is treated in a rather approximate way by extrapolation from upstream density distributions. This may explain why agreement with experiments is worst for the lowest Froude number case (run 3).

5. Conclusions

The paper has described a new mathematical model for the calculation of a three-dimensional heated surface jet in stagnant surroundings. The model is of the finite-difference type and does not therefore require any assumptions about profile shapes as in integral-type models; unlike other numerical models however it does not solve the full three-dimensional elliptic equations and is therefore considerably more economical. In contrast to all previously suggested models the handling of turbulence in the present

† Unfortunately, there are no lateral velocity profiles available for runs 1 and 2.

scheme rests on a physically much sounder basis, namely the use of simplified forms of the modelled equations governing the transport of Reynolds stresses and turbulent heat fluxes. In this way, the effect of buoyancy on the turbulent transport terms is obtained much less empirically than in other models; in fact the reduction of jet entrainment due to buoyancy is an outcome and not an imput. It should also be stressed here once more that none of the empirical constants in the turbulence equations were altered for the present flow problem.

The experiments of Pande & Rajaratnam for this flow were adjudged to be superior to those of other investigators and were used therefore to assess the performance of the model. The agreement with these measurements was in general acceptable over the major portion of the flow, the discrepancies near the edges of the jet being difficult to assess, since, although these experiments reproduce the discharge into infinite surroundings over a large part of the flow, near the jet edges the data are suspect due to the use of a finite size tank. In these jet edge regions also the use of a quasi-orthogenal grid system spreading at such large angles probably leads to some inaccuracies. After comparison with the measurements the model predictions were then used to explain and clarify certain phenomena observed in the experiments, for example the undulatory behaviour of the half-width and the differing shapes of velocity and temperature profiles in the horizontal and vertical directions.

The limitations of the model should also be discussed here; the first restriction which has been made is that the model in its present form is only valid for the jet region of the flow and is not applicable to the stratified spreading layer region outside the jet. Rather than extend the model to deal with this problem however, removal of other limitations should take higher priority in order to extend the applicability of the model. Two extensions are worthy of mention, since they are comparatively easy to include. Firstly it is possible to modify the model for the case of discharge over a sloping bottom. In this case the surface elevation terms in the momentum equations cannot be removed as in the present model and must be calculated explicitly. When the jet remains attached to the bottom however, both bottom and surface vertical velocities are known to be zero and it is possible to calculate the pressure gradients due to surface inclination from a guess-and-correct procedure (similar to the pressure correction approach of Patankar & Spalding 1972); this would employ the fact that continuity must be satisfied over vertical columns of cells. The second limitation which can be removed is to make the model applicable to jet discharges into a mild cross-flow. For such problems the present model can be combined with equations similar to those used in some integral models where the jet bending due to pressure forces and entrainment of ambient cross-flow momentum is calculated. Only the drag force due to pressure differences across the jet would require further empirical input, an effect which is relatively unimportant, compared to bending due to ambient fluid entrainment, according to Dunn *et al.* (1975). The mathematical model could then be applied to a wide range of practical discharge problems.

The calculations were carried out on the UNIVAC 1108 computer of the University of Karlsruhe using a modified version of the program STABLE of CHAM Ltd, London, which is based on the solution algorithm of Patankar & Spalding (1972).

REFERENCES

BATCHELOR, G. K. 1967 *An Introduction to Fluid Dynamics.* Cambridge University Press.

CHU, V. H. & VANVARI, M. R. 1976 Experimental study of turbulent stratified shearing flow. *J. Hydraul. Div. A.S.C.E.* **102**, (HY6), 691–706.

DEMUREN, A. D. & SPALDING, D. B. 1977 Mathematical modelling of steady two-dimensional surface flows. *Dept. Mech. Engng, Imp. Coll. Rep.* HTS/77/23.

DUNN, W. E., POLICASTRO, A. J. & PADDOCK, R. A. 1975 Surface thermal plumes; evaluation of mathematical models for the near and complete field. *Argonne National Laboratory Rep.* ANL/WR-75-3.

ELLISON, T. H. & TURNER, J. S. 1959 Turbulent entrainment in stratified flows. *J. Fluid Mech.* **15**, 413–448.

ENGELUND, F. 1976 Hydraulics of surface buoyant jet. *J. Hydraul. Div. A.S.C.E.* 102 (HY9), 1315–1325.

GIBSON, M. M. & LAUNDER, B. E. 1976 On the calculation of horizontal, turbulent free shear flow under gravitational influence. *Trans. A.S.M.E., J. Heat Transfer*, C**98**, 81–87.

HAYASHI, T. & SHUTO, N. 1967 Diffusion of warm water jets discharged horizontally at the water surface. *12th Cong. IAHR, Fort Collins, Colorado, U.S.A.*

HOSSAIN, M. S. 1979 Mathematische Modellierung von turbulenten Auftriebsströmungen. Ph.D. thesis, University of Karlsruhe.

HOSSAIN, M. S. & RODI, W. 1977 Influence of buoyancy on the turbulence intensities in horizontal and vertical jets. In *Heat Transfer and Turbulent Buoyant Convection: Studies and Applications for Natural Environment, Buildings, Engineering Systems*, vol. 1 (ed. D. B. Spalding & N. Afgan). Washington, D.C.: Hemisphere Publishing Corp.

JIRKA, G. H., ABRAHAM, G. & HARLEMAN, D. R. F. 1975 An assessment of techniques for hydrothermal prediction. Ralph M. Parsons Laboratory for Water Resources and Hydromechanics, *MIT Rep.* no. 203.

LAUNDER, B. E. 1975 On the effect of a gravitational field on the turbulent transport of heat and momentum. *J. Fluid Mech.* **67**, 569–587.

LAUNDER, B. E. 1976 Progress in the modelling of turbulent transport. *Lecture Series* 76. von Kármán Institute.

LAUNDER, B. E. & SPALDING, D. B. 1974 The numerical computation of turbulent flows. *Comp. Meth. in Appl. Mech. & Eng.* **3**, 269–289.

LAUNDER, B. E., REECE, G. J. & RODI, W. 1975 Progress in the development of a Reynolds stress turbulence closure. *J. Fluid Mech.* **68**, 537–566.

MCGUIRK, J. J. & RODI, W. 1977 Calculation of three-dimensional heated surface jets. In *Heat Transfer and Turbulent Buoyant Convection: Studies and Applications for Natural Environment, Buildings, Engineering Systems*, vol. 1 (ed. D. B. Spalding & N. Afgan). Washington, D.C.: Hemisphere Publishing Corp.

MCGUIRK, J. J. & RODI, W. 1979 The calculation of three-dimensional turbulent free jets. In *Turbulent Shear Flows* I (ed. F. Durst, B. E. Launder, F. W. Schmidt & J. H. Whitelaw). Springer.

PANDE, B. B. LAL & RAJARATNAM, N. 1975 An experimental study of heated surface discharges into quiescent ambients. *Tech. Rep. Dept. of Civil Engng*, The University of Alberta, Edmonton, Canada. 1977 partly published in *J. Hydraul. Res.* **15**, 261–275.

PATANKAR, S. V. & SPALDING, D. B. 1972 A calculation procedure for heat, mass and momentum transfer in three-dimensional parabolic flows. *Int. J. Heat Mass Transfer* **15**, 1787–1806.

PAUL, J. 1973 A numerical model for a three-dimensional, variable-density jet, doctoral dissertation. *Dept. Fluid, Thermal and Aerospace Science*, Case Western Reserve University.

RODI, W. 1978 Turbulence models and their application in hydraulics – a state of the art review. *University of Karlsruhe Rep.* SFB 80/T/127.

SHARMA, D. 1974 Turbulent convective phenomena in straight, rectangular-sectional diffusers. Ph.D. Thesis, University of London.

SHIRAZI, M. 1973 Pacific Northwest Environmental Research Laboratory Working Paper No. 4, U.S.E.P.A., Corvallis, Oregon, U.S.A.

SHIRAZI, M. & DAVIS, L. E. 1976 Analysis of buoyant surface jets. *Trans. A.S.M.E., J. Heat Transfer* 367–372.

STEFAN, H. & SCHIEBE, F. R. 1970 Heated discharge from flume into tank. *J. Sanitary Engng. Div. A.S.C.E.* **96** (SA6), 1415–1433.

STEFAN, H. & VAIDYARAMAN, P. 1972 Jet-type model for the three-dimensional thermal plume in a cross current underwind. *Water Resources Res.* **8**, 4.

STOLZENBACH, K. D. & HARLEMAN, D. R. F. 1971 An analytical and experimental investigation of surface discharges of heated water. Ralph M. Parsons Laboratory for Water Resources and Hydrodynamics, *MIT Rep.* no. 135.

WALDROP, W. & FARMER, R. 1974 Three-dimensional computation of buoyant plumes. *J. Geophys. Res.* **79**, 9.

WIUFF, R. 1978 Experiments on surface buoyant jet. *J. Hydraul. Div. A.S.C.E.* **104** (HY5), 667–679.